Geophys. J. R. astr. Soc. (1986) **84,** 413–430

Linear programming approach to moment tensor inversion of earthquake sources and some tests on the three-dimensional structure of the upper mantle

Toshiro Tanimoto and Hiroo Kanamori *Seismological Laboratory, California Institute of Technology, Pasadena, California 91125, USA*

Accepted 1985 July 12. Received 1985 July 12; in original form 1984 December 11

Summary. A new method of moment tensor inversion is developed, which combines surface wave data and *P*-wave first motion data in a linear programming approach. Once surface wave spectra and first motion data are given, the method automatically obtains the solution that satisfies first motion data and minimizes the L1 norm of the surface wave spectra. We show the results of eight events in which the method works and is stable even for shallow events. We also show one event in which surface wave data and *P*-wave first motion data seem to be incompatible. In such cases, our method does not converge or converges to a solution which has a large minor (second) double couple component. It is an advantage that the method can determine the compatibility of two data sets without trial and error.

Laterally heterogeneous phase velocity corrections are used to obtain spectra at the source. The method is also applied to invert moment tensors of eight events in two recent three-dimensional (3-D) upper mantle structures. In both 3-D models, variances of spectra are smaller than those in a laterally homogeneous model at 256 s. Statistical tests show that those reductions are significant at a high confidence level for five events out of eight examined. For three events, we examined those reductions at shorter periods, 197 and 151 s. The reduction of variances is comparable to the results at 256 s and is again statistically significant at a high confidence level. Orientation of fault planes does not change very much by incorporation of lateral variations of phase velocity or by doing inversions at different periods. This is mainly because of the constraints from *P*-wave first motion data. Scatter of phase spectra at shorter periods, especially at 151 s, is great and suggests that surface wave ray paths deviate from great circle paths substantially and these effects cannot be ignored.

Key words: inversion, moment, tensor

Downloaded from http://gji.oxfordjournals.org/ at California Institute of Technology on November 7, 2014

1 Introduction

One of the aims of this paper is to present a method to invert for the moment tensor of an earthquake source by combining surface wave data and *P*-wave first motion data in a linear programming approach. The indeterminacy of moment tensors of shallow earthquakes, if only long-period surface waves are used, is well known (e.g. Trehu, Nabelek & Solomon 1981; Kanamori & Given 1981). In order to circumvent this problem, information from shorter period data must be incorporated. Body wave modelling (e.g. Dziewonski & Woodhouse 1983) represents one approach to this problem, although the indeterminacy cannot be completely removed for shallow events. We attempt to resolve this problem by adding *P*-wave first motion data to surface wave spectral data. This approach has been discussed by Michael & Geller (1984), Nakanishi & Kanamori (1984), Kanamori (1983) and Scott & Kanamori (1985). These papers attempted to obtain some information on the orientation of fault planes from first motion data and used that additional information to remove the ambiguities of surface wave inversion. One of the problems associated with these studies is that first motion data do not necessarily provide any unique information.

In this paper, we discuss a method that combines the two data sets in a very natural way; it seeks the minimum L1 norm solution for the surface wave spectral data, while satisfying the first motion data. Some advantages of the approach over the others are (1) the whole process is automated and (2) the criterion for selecting a particular solution (i.e. the L1 norm) becomes objective.

The second aim of this paper is, by using the method presented here, to do the moment tensor inversions of earthquakes in two recent 3-D upper mantle models; one by Woodhouse & Dziewonski (1984) and another by Tanimoto (1985). We apply laterally heterogeneous phase velocity corrections based on these two models to obtain spectra at the source. We examine how incorporation of these effects affect the solutions and how well the two models can improve the inversion results.

2 Method

2.1 BASIC FORMULA

In this paper, we consider Rayleigh waves in a vertical component seismogram at one frequency only. From one measurement of surface wave spectra, we obtain

$$A_1 M_{xy} + A_2(-M_{xx} + M_{yy}) + A_3(M_{xx} + M_{yy}) + A_4 M_{yz} + A_5 M_{xz} = V_r \qquad (1)$$

where, in the notation of Kanamori & Given (1981),

$$A_1 = -P_R^{(1)} \sin 2\phi$$

$$A_2 = \frac{1}{2} P_R^{(1)} \cos 2\phi$$

$$A_3 = -\frac{1}{2} S_R^{(1)}$$

$$A_4 = iQ_R^{(1)} \sin \phi$$

$$A_5 = iQ_R^{(1)} \cos \phi$$

Downloaded from http://gji.oxfordjournals.org/ at California Institute of Technology on November 7, 2014

and V_r is the spectrum propagated from the observed station back to the earthquake source (Kanamori & Given 1981) assuming a certain earth structure. We take the same coordinate system as Kanamori & Given (1981). The trace of the moment tensor is constrained to be zero in this formula, i.e. $M_{xx} + M_{yy} + M_{zz} = 0$. From the real and imaginary parts of (1), we obtain two equations. Thus for n observations of spectra, we get $2n$ equations. In matrix form, we write them as

$$AM = V, \tag{2}$$

where A and V are the same as equation (7) in Kanamori & Given (1981), and

$$M = (M_{xy}, -M_{xx} + M_{yy}, M_{xx} + M_{yy}, M_{yz}, M_{xz})$$
$$\equiv (M_1, M_2, M_3, M_4, M_5).$$

From observations of P-wave first motion data, we obtain

$$C^t M > 0 \quad \text{for compression,}$$

$$C^t M < 0 \quad \text{for dilatation,}$$

$$C^t M \approx 0 \quad \text{for near nodal stations,} \tag{3}$$

where

$$C^t = [\sin^2 i \sin 2\phi, -\frac{1}{2}\sin^2 i \cos 2\phi, \frac{1}{2}(1 - 3\cos^2 i), -\sin 2i \sin \phi, -\sin 2i \cos \phi]$$

with ϕ denoting the azimuth and i the take-off angle of P-waves at the source.

If we combine (2) and (3), we obtain a typical linear programming problem: that is to minimize

$$\sum_i \sum_{j=1}^{5} |A_{ij}M_j - V_i| \tag{4}$$

with constraints

$$\sum_i C_i M_i > 0. \tag{5}$$

Dilatational data are multiplied by -1 to be positive constraints. The minimization function (4) contains equations for near nodal points in (3).

2.2 ALGORITHM

The problem given in (4) and (5) is a linearly constrained problem in optimization theory and is already studied in detail (e.g. Luenberger 1984). The most recent summary in this kind of problem, i.e. the least L1 norm problem, is Bloomfield & Steiger (1984). There are basically two approaches to this kind of problem. One is the simplex method. Armstrong & Hultz (1977) presented an algorithm for the L1 norm problem by the simplex method. The other method is the one that transforms the problem to an unconstrained minimization problem by forming a function which combines (4) and (5), and searches for its minimum by looking for a descent direction in a multi-dimensional parameter space. Bartels & Conn (1980) gave an algorithm using this method.

Downloaded from http://gji.oxfordjournals.org/ at California Institute of Technology on November 7, 2014

We chose the latter algorithm for our problem, mainly because the method does not require a feasible point to start. A feasible solution is a solution which satisfies all constraints. In most cases, we do not know from the outset whether there exists a fault plane solution which satisfies a given *P*-wave first motion data set or not. Thus, in the former method, we must be careful in selecting the initial fault plane solution, while in the latter method, we do not have to be so careful on this point. It is quite easy to automate the whole procedure by the latter method.

For details, one should consult the papers by Bartels & Conn (1980) and Conn & Pietrzykowski (1977), but we briefly outline how the algorithm works. We form the following function

$$\phi(M_1, M_2, \ldots, M_5) = \gamma \sum_i \sum_{j=1}^{5} |A_{ij}M_j - V_i| - \sum_k \min(0, C_k^t M) \tag{6}$$

where C_k is the vector in (3) for the kth datum and γ is called the penalty parameter. The penalty parameter γ is initially set to 1 and the method seeks a minimum of ϕ as a function of moment tensor elements, $M_1, \ldots, M_5$. The method lowers γ and seeks a minimum of such ϕ. Conn & Pietrzykowski (1977) showed that if the problem given in (4) and (5) has a solution, there exists a threshold $\bar{\gamma}$ such that for all $0 < \gamma \leqslant \bar{\gamma}$ the minimum of (6) provides a solution to the problem. The method examines a few values of γ to find a solution. In most cases, the minimum found for $\gamma = 1$ turned out to be the solution.

3 Data

We show the results of nine earthquakes in Table 1. We list the origin times and hypocentre locations from NEIS (National Earthquake Information Service). Earthquakes denoted by K4, S12, N17, L22, C24 and A25 were analysed by Kanamori & Given (1981) and also by Nakanishi & Kanamori (1984). Three earthquakes were in North America, three in the South Pacific and one from each of the following regions: north-western Pacific, Nepal and south of Africa. Source process times were determined by searching for the minimum residual of surface wave spectra at 256 s in the moment tensor inversion. This is the correction from the non-directional part of the finite source process and we use the same definition as in Nakanishi & Kanamori (1984). At present the directional part is hard to recover from the data set.

Table 1. Events analysed. Data from NEIS.

Event	M	D	Y	H	M	S	Longitude	Latitude	Depth(Km)	* (sec)	
Coalinga	5	2	83	23	42	37.8	36.233N	120.293W	10.5	20	Coalinga
Idaho	10	28	83	14	6	22.5	44.030N	113.914W	16.0	40	Borah Peak
K4	2	23	80	5	51	3.2	43.530N	146.753E	44.0	20	Kuril
S12	7	8	80	23	19	19.8	12.410S	166.381E	33.0	50	Santa Cruz Is.
N17	7	29	80	14	58	40.8	29.598N	81.092E	18.0	15	Nepal
L22	10	25	80	11	0	5.1	21.890S	169.853E	33.0	45	Loyalty Is.
C24	11	8	80	10	27	34.0	41.117N	124.253W	19.0	30	N. California
A25	11	11	80	10	36	58.2	51.422S	28.796E	10.0	30	South of Africa
P18	9	26	80	15	20	37.1	3.225S	142.237E	33.0	15	Papua

* Source process time

Downloaded from http://gji.oxfordjournals.org/ at California Institute of Technology on November 7, 2014

4 Homogeneous earth model

In this section, we report the results in a laterally homogeneous earth and show how the method presented in Section 2 was performed. We restrict ourselves to the case of a 256 s period for surface wave spectra and use the earth model PREM (Dziewonski & Anderson 1981) to propagate the observed phase back to the source. The attenuation correction was also done by using PREM and the geometric spreading correction was done by using the asymptotic normal mode theory as, for example, in Kanamori & Given (1981).

4.1 STARTING SOLUTIONS

The linear programming algorithm is an iterative method. Since the problem is linear, one might expect not to have to worry about the starting point. The following example illustrates that this is not so: take, for example, a function $\phi(x) = |x| + |x - 1|$. This function has a flat region of minimum between $x = 0$ and 1. If we start from $x = 2$, we obtain the solution $x = 1$ and if we start from $x = -1$, we get the solution $x = 0$. This is, of course, a special case, since the first and the second term have the same coefficient of x, which is 1. But it can happen within a finite number of digits in a computer. In order to circumvent this problem to a certain extent, we tried two different starting points in every case and examined whether they converge to the same solution. One starting solution is the constrained moment tensor solution ($M_{yz} = M_{xz} = 0$), advocated by Kanamori & Given (1981) for rapid determination of earthquake sources. The other starting solution is the body wave solution obtained from the inversion of *P*-wave first motion data (Kanamori 1983). The latter solution is obtained in the following way: for one observation of *P*-wave first motion, we obtain

$$u = C^{t}M$$

where u is the amplitude and C and M are vectors defined in Section 2. It is very difficult to measure u from the observed data, and therefore we put $u = +1, 0$ and -1 for compression, nodal and dilatation and solve such equations by the least-squares method. This is a very crude approach but, as the following results show, we can obtain a fault plane solution which satisfies *P*-wave first motion data very well. The solution is good enough for the starting point in our iterative procedure.

4.2 EXAMPLES

Fig. 1(a–d) show the two starting and the final solutions of four events: K4, S12, L22 and A25. In each case, the left figure is the constrained moment tensor solution, the middle the body wave starting solution, and the right the final solution. In all events we report in this paper, two starting solutions converged to the same solution. Note that the constrained moment tensor solutions violate many points in *P*-wave first motion data set, while the body wave solution matches *P*-wave first motion data quite well. Nonetheless, the final solutions are not necessarily close to the body wave starting solution. Final solutions of Coalinga, N17 and C24 are shown in Fig. 2. The final solution of the Idaho earthquake is shown in Fig. 3 and is denoted by HOMO.

Fault parameters of the major double couples are given in Table 2. Rows specified by HOMO are the solutions in a laterally homogeneous case and $(\delta_1, \lambda_1, \phi_1)$ and $(\delta_2, \lambda_2, \phi_2)$ are dip angle, slip angle and strike of the first and second fault planes. In the fourth row of each earthquake, we included the results by other researchers (in a laterally homogeneous

Downloaded from http://gji.oxfordjournals.org/ at California Institute of Technology on November 7, 2014

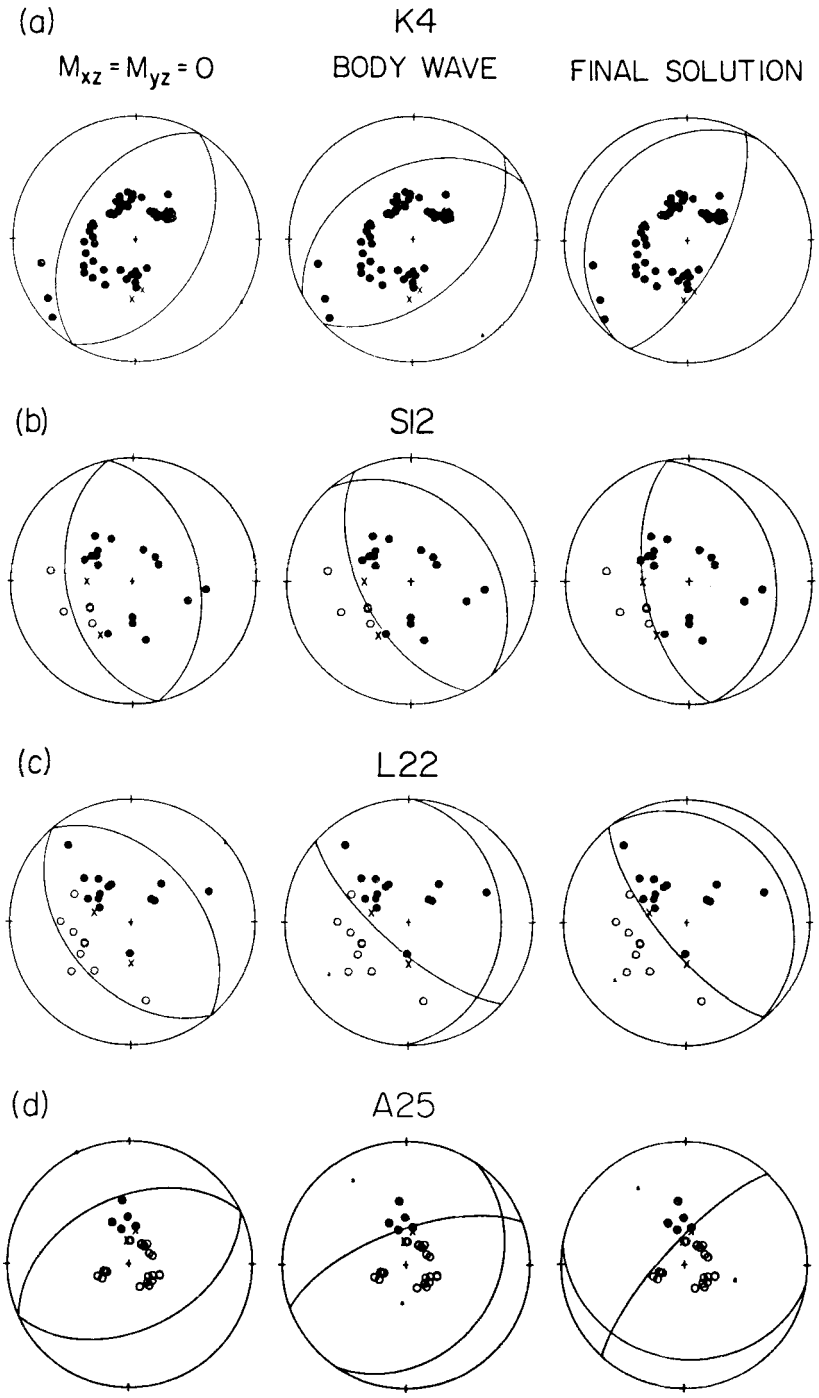

Figure 1. (a–d) Two initial models and the final focal mechanism solution. Both initial models converge to the same final solution. Two initial solutions are (1) the constrained moment tensor solution and (2) the body wave solution which is obtained by inverting the *P*-wave first motion data. K4, S12, L22 and A25 correspond to events listed in Table 1. First motion data are denoted by black circles and open circles corresponding to compression and dilatation respectively.

Downloaded from http://gji.oxfordjournals.org/ at California Institute of Technology on November 7, 2014

Table 2. Solutions at 256 s.

		1	1	1	2	2	2	Mo (10^{27} cgs)	Minor/Major[7] (%)
Coalinga	HOMO[1]	66	72	-64	30	125	165	0.056	7.2
	HVD[2]	66	78	-66	27	115	152	0.058	2.7
	BG[3]	65	75	-66	29	119	156	0.056	1.1
	K[4]	65	70	-58	32	126	163	0.054	
Idaho	HOMO	39	-67	140	55	-108	-69	0.36	10.7
	HVD	48	-61	146	49	-119	-74	0.38	4.7
	BG	49	-59	150	50	-121	-72	0.34	0.2
	DFW[5]	62	-83	138	29	-103	-56	0.31	5.6
K4	HOMO	65	94	35	26	81	-155	0.73	6.3
	HVD	62	96	40	29	78	-154	0.65	1.7
	BG	70	88	29	20	95	-146	0.84	2.1
	NK[6]	70	89	27	20		-151	0.63	
S12	HOMO	31	89	-11	60	91	170	2.4	2.3
	HVD	31	86	-15	59	93	170	2.4	1.9
	BG	31	88	-13	59	92	170	2.4	1.9
	NK	31		-16	59	93	170	2.2	
N17	HOMO	69	99	117	23	67	-88	0.092	3.5
	HVD	55	119	128	44	56	-95	0.074	4.1
	BG	69	98	18	23	70	-84	0.101	6.6
	NK	70	90	111	20		-69	0.083	
L22	HOMO	18	92	-37	72	89	141	2.9	0.4
	HVD	18	85	-40	73	92	146	3.1	0.9
	BG	17	93	-33	73	89	144	3.1	2.6
	NK	17		-32	73	88	142	2.9	
C24	HOMO	88	177	141	87	2	232	1.2	2.0
	HVD	83	178	142	88	7	232	1.3	1.7
	BG	82	178	142	88	8	232	1.3	2.4
	NK	90		140	90	0	230	1.0	
A25	HOMO	79	-111	-142	24	-30	100	0.32	6.1
	HVD	78	-110	-144	23	-32	98	0.36	7.9
	BG	79	-111	-142	24	-30	100	0.32	6.8
	NK	78	-112	-137	25		115	0.32	
P18	HOMO	44	48	113	59	123	-16	0.20	35.8
	NK	42		107	72	129	-4	0.17	

(1) Spherically symmetric earth.
(2) Phase velocity corrected by Harvard model (Woodhouse & Dziewonski 1984).
(3) Phase velocity corrected by BG80 (Tanimoto 1985).
(4) Kanamori (1983).
(5) Dziewonski *et al.* (1984).
(6) Nakanishi & Kanamori (1984).
(7) Ratio of the smallest eigenvalue to the largest one in the moment tensor matrix, given in per cent.

earth). It seems common to find the differences of 5° in dip and slip angles and of 10° in strike directions among the results of different studies. Differences in moment are up to 20 per cent for these events.

In the rightmost column of Table 2, we listed the ratios of minor to major double couples. This is the ratio of the smallest to largest eigenvalues of the moment tensor and is given in per cent. They are generally less than 10 per cent, much less than those given in Kanamori & Given (1981). As the orientation of the fault is better constrained, these ratios seem to become less and less and the solution becomes closer to a double couple source. But a few to 10 per cent seems to be the limit of present accuracy. Thus, it is probably impossible to prove or disprove the existence of compensated linear vector dipole of less than 10 per cent at present.

Downloaded from http://gji.oxfordjournals.org/ at California Institute of Technology on November 7, 2014

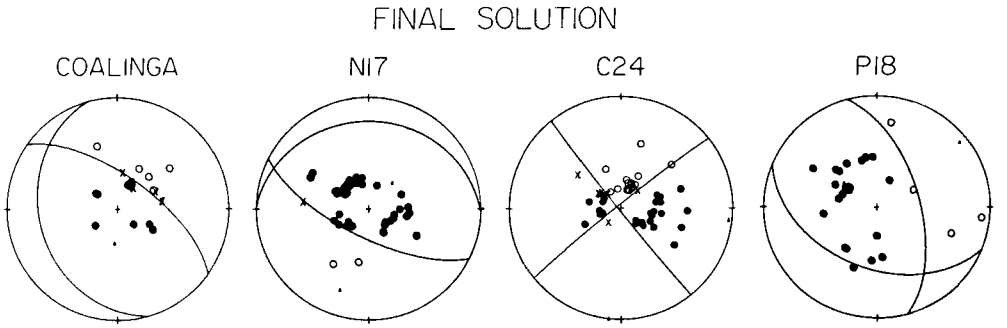

Figure 2. Final solutions of Coalinga, N17, C24 and P18. The final solution of the Idaho (Borah Peak) event is shown in Fig. 3, denoted by HOMO. For P18 note that two data are violated by the major double couple, but the large minor double couple distorts nodal lines such that these data are not violated.

Although it has been a rare occurrence, surface wave and *P*-wave first motion data did not seem to be compatible for some events. One of them is the last event in Table 1, an earthquake in Papua (P18). In such a case, our method shows a problem of convergence or converges to a solution which has a substantial minor double couple component; for P18, the solution converged, but the minor double couple component amounted to 35.8 per cent of the major double couple component. Fig. 2 shows the final solution for this event. Nodal lines are those for the major double couple component. Two first motion data, one compression and one dilatation, apparently violate the major double couple solution. They do not violate the total solution, the sum of major and minor double couples, because the minor double couple is large and the nodal lines deviate from the ones shown in Fig. 2.

The way the method works in such a situation can be looked upon as follows. We take the case of a body wave starting solution. In this case the starting solution satisfies *P*-wave first motion data and is a double couple source. But its residual of surface wave spectral data is not at its minimum. For many events, the minimum of the surface wave residual is close to that starting solution and the method converges to the solution quickly. However, when surface wave data and *P*-wave first motion data are incompatible, the minimum is very far and cannot be reached without violating first motion data. In some cases, if the minor double couple is allowed to become large, the solution can even come closer to the minimum of surface wave residual without violating first motion data, because nodal line distortions can take account of violations of the major double couple as shown in Fig. 2.

One can think of a few reasons why surface wave data and *P*-wave first motion data become incompatible. If it is a true incompatibility, it may have been caused by a non-planar fault or a real non-double couple source. But it can also be an artefact of assumptions in the analysis like the effect of the near source anomaly on the *P*-wave take-off angle estimation (e.g. Solomon & Julian 1974), and the effect of inaccurate source depths used for surface wave excitation function calculations. The problems of source depths can be circumvented by trying different depths, which we did for all events in this paper. But other cases cannot be distinguished in the present analysis. For P18, the use of average excitation function between the depths of 0 and 53 km helped to reduce the residual of surface wave spectra (Nakanishi & Kanamori 1984), but the minor double couple remained large (30 per cent) by our method. Since regions near Papua seem to be complicated, in that many earthquakes have quite different focal mechanisms (Kanamori & Dziewonski 1984), this earthquake may have had a substantial non-planar fault but this is still inconclusive from our analysis.

Downloaded from http://gji.oxfordjournals.org/ at California Institute of Technology on November 7, 2014

5 Heterogeneous earth models: phase velocity correction

The importance of the accuracy of phase velocities in the moment tensor inversion has been emphasized by many researchers, especially for waves with periods below 100 s. Corrections for lateral heterogeneity have been made for such cases (Aki & Patton 1978; Patton 1980; Trehu *et al.* 1981). Even for long-period waves of about 250 s, some efforts have been made to correct for lateral heterogeneity (Nakanishi & Kanamori 1982) using regionalized earth models. In this section, we discuss the effects of phase velocity correction using two recent 3-D upper mantle models: one is by Woodhouse & Dziewonski (1984, hereafter HVD) and the other by Tanimoto (1985, 1986, hereafter BG80). The latter was recently obtained by applying the Backus–Gilbert method to the data set of measured phase velocities. The main purposes are to examine how large phase corrections are by these models and how they affect the moment tensor inversion. We examined these points mainly at 256 s, but for three events, we also analysed them at 197 and 151 s. It is also of interest to compare which earth model, HVD or BG80, produces less variances in the moment tensor inversions. Phase velocities of each model, expanded in spherical harmonics, are tabulated in Table 5. First we discuss the results at 256 s and then the results at 197 and 151 s.

5.1 RESULTS AT 256 S

Fig. 3 shows our focal mechanism solutions of the Idaho (Borah Peak) earthquake with the solution by Dziewonski, Franzen & Woodhouse (1984), denoted by DFW. The solution

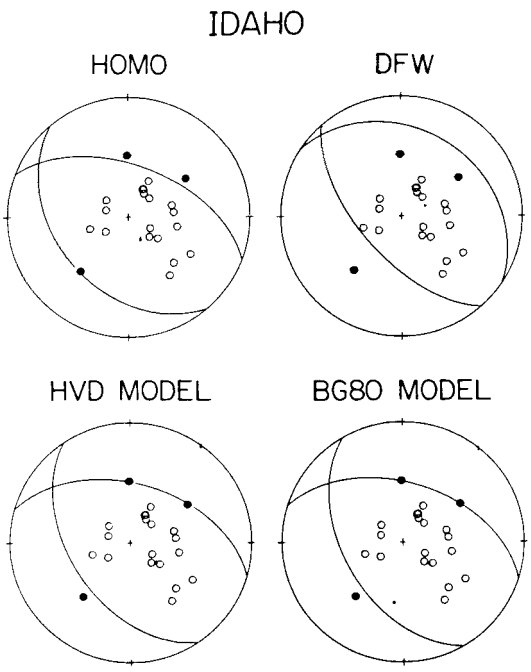

Figure 3. Solutions of the Idaho event in a laterally homogeneous earth (HOMO) and in two laterally heterogeneous earth models, HVD and BG80. The solution denoted by DFW is the one by Dziewonski *et al.* (1984).

Downloaded from http://gji.oxfordjournals.org/ at California Institute of Technology on November 7, 2014

Table 3. Reduction of residuals at 256 s.

Event	Period		f	2N	75%	90%	95%	99%
K4	256	HVD	1.10	42	X	X	X	X
		BG80	1.12	42	X	X	X	X
S12	256	HVD	1.02	42	X	X	X	X
		BG80	1.28	42	O	X	X	X
N17	256	HVD	2.16	34	O	O	O	X
		BG80	1.80	34	O	O	O	X
L22	256	HVD	1.06	48	X	X	X	X
		BG80	1.23	48	O	X	X	X
A25	256	HVD	2.07	86	O	O	O	O
		BG80	1.46	86	O	O	X	X

denoted by HOMO is the one for the laterally homogeneous case (PREM). HVD and BG80 are the cases with phase velocity corrections using corresponding models. Note that HOMO, HVD and BG80 are our solutions using surface waves at 256s, while DFW is the one at a broader period range by waveform inversion in the time domain. One important aspect of this figure is that the differences between HOMO and HVD or between HOMO and BG80 are not as great as the differences between HOMO and DFW. In other words, the differences

Table 4. Reduction of residuals at 256, 197 and 151 s.

Event	Period		f	2N	75%	90%	95%	99%
Coalinga	256	HVD	1.85	66	O	O	O	O
		BG80	1.14	66	X	X	X	X
	197	HVD	2.25	66	O	O	O	O
		BG80	1.66	66	O	O	O	X
	151	HVD	2.10	66	O	O	O	O
		BG80	2.07	66	O	O	O	O
Idaho	256	HVD	3.76	74	O	O	O	O
		BG80	2.22	74	O	O	O	O
	197	HVD	2.34	74	O	O	O	O
		BG80	2.62	74	O	O	O	O
	151	HVD	1.64	74	O	O	O	X
		BG80	1.64	74	O	O	O	X
C24	256	HVD	2.31	44	O	O	O	O
		BG80	2.82	44	O	O	O	O
	197	HVD	2.19	44	O	O	O	O
		BG80	3.57	44	O	O	O	O
	151	HVD	1.88	44	O	O	O	X
		BG80	2.96	44	O	O	O	O

Downloaded from http://gji.oxfordjournals.org/ at California Institute of Technology on November 7, 2014

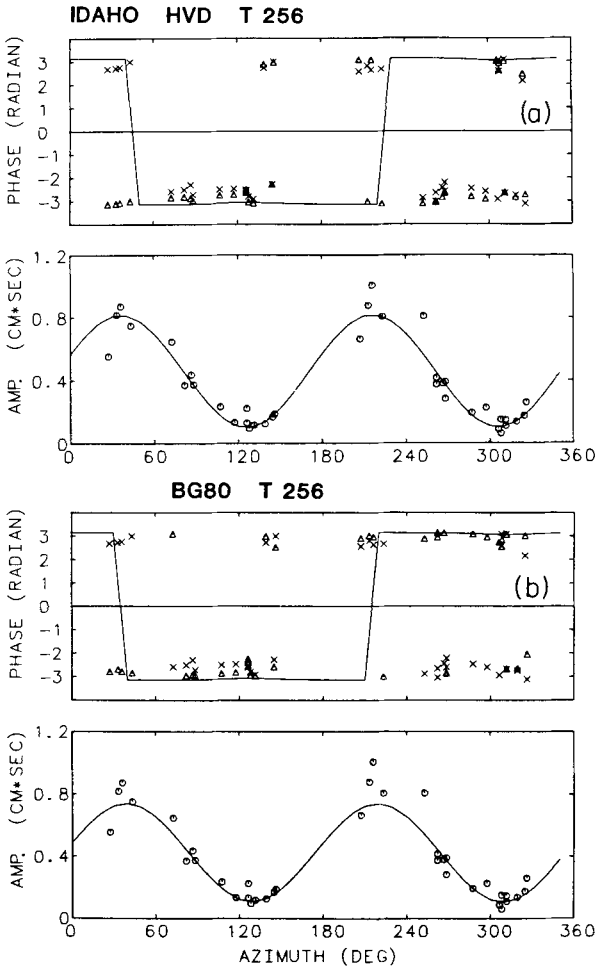

Figure 4. (a, b) Phase and amplitude of source spectra of Idaho events at 256 s. The top figure corresponds to phase and the bottom to amplitude. The data x in the phase figure are obtained by using a laterally homogeneous earth model (PREM) and the data Δ by the laterally heterogeneous models HVD (a) and BG80 (b). Solid lines are the theoretical curves for the final solution in an heterogeneous case. For shallow, dip-slip dominated events, phases are either $-\pi$ or π and thus corrections by heterogeneous models are moving those phase data in the right direction.

between different methods (or studies) are bigger than the effects of phase velocity corrections by laterally heterogeneous models at present.

Table 2 also gives the moment of each solution. We used the largest eigenvalue for this. Nakanishi & Kanamori (1982) discussed that the phase errors may cause a bias to low scalar moments. It is generally true that as theoretical wave trains become more in phase with observed wave trains, due for example to the corrections by lateral heterogeneity, the moment becomes greater. However, this is true to the extent that the orientation of the fault does not change much by its effect.

In a few cases, if we use laterally heterogeneous models, the orientation of the solution is affected, resulting in a smaller moment value than that of an homogeneous case. A few such cases are seen in Table 2. But the majority of results seems to be in the increasing trend. This

Downloaded from http://gji.oxfordjournals.org/ at California Institute of Technology on November 7, 2014

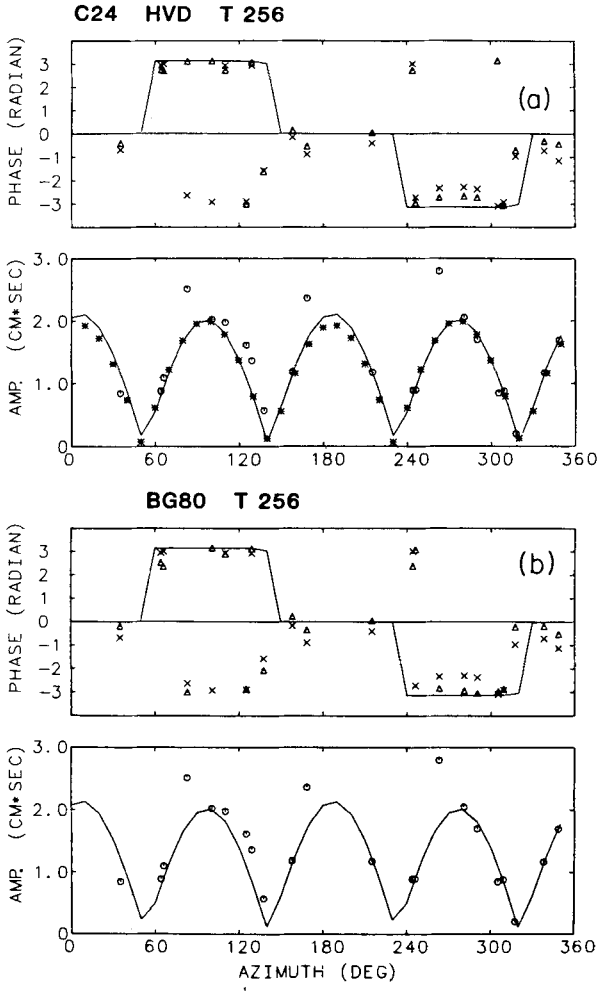

Figure 5. (a, b) Same as Fig. 4 except for a different event, C24. This event is predominantly strike-slip and the initial phase should be $-\pi$, 0 or π. Again most corrections are systematic and seem to be in the right direction. Stars * in (a) are the theoretical prediction of the final solution in the homogeneous case.

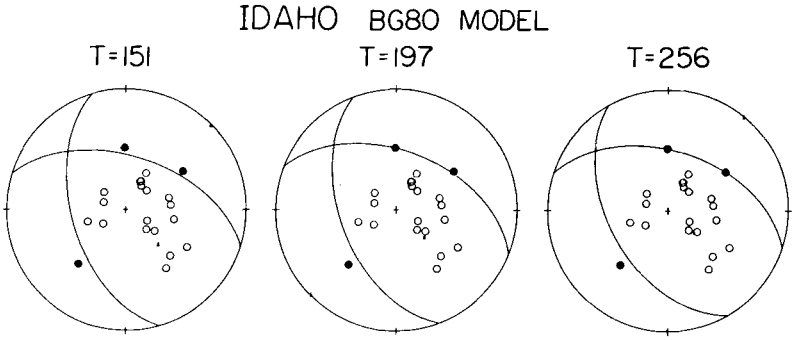

Figure 6. Final solutions of the Idaho events at three different frequencies, 151, 197 and 256 s. Laterally heterogeneous phase velocity corrections by BG80 are applied in all cases. There is a difference of 5–10° in dip, slip and strike directions, but the differences among them are not as great as the differences between different methods (e.g. DFW in Fig. 3).

Downloaded from http://gji.oxfordjournals.org/ at California Institute of Technology on November 7, 2014

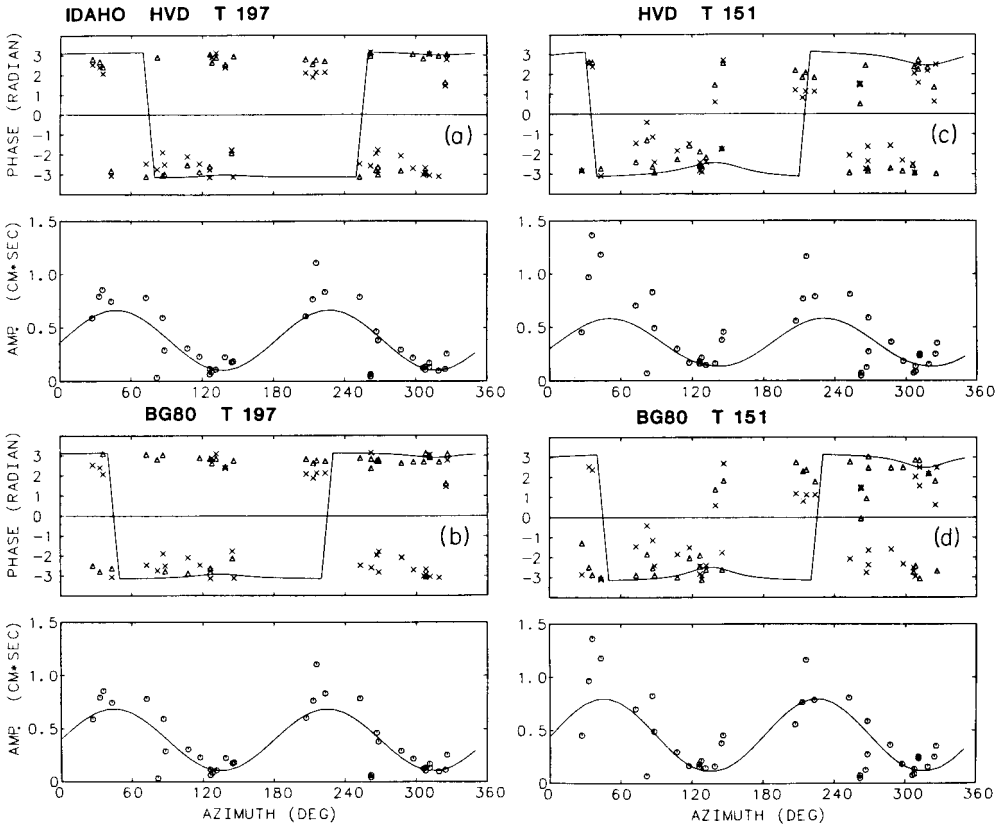

Figure 7. (a–d) Phase and amplitude of Idaho events at 197 s (a and b) and at 151 s (c and d). (a) and (c) are corrected by HVD and (b) and (d) by BG80. Corrections in phase are substantial and seem to be in the right direction for most data, but the scatter of data seems to increase for shorter periods. At 151 s, surface wave ray paths may be deviating from great circle paths substantially.

argument, of course, can be complicated further, by the size (magnitude) of minor double couples, which are different in every case (Table 2).

We can measure how much a laterally heterogeneous model can improve the inversion process by the following quantity:

$$f = \frac{\epsilon^2_{\mathrm{HOM}}}{\epsilon^2_{\mathrm{HET}}}$$

where $\epsilon^2_{\mathrm{HOM}}$ is the variance in an homogeneous case and $\epsilon^2_{\mathrm{HET}}$ the variance in an heterogeneous case. They are both calculated in the L2 norm after we obtained the solutions. The value of f in each case is tabulated in Tables 3 and 4. For five events in Table 3, the results at 256 s are given and for the other three events in Table 4, the results at different periods 197 and 151 s, are also given. Numbers given under $2n$ are twice the number of observations or the number of equations in (2). Degrees of freedom are given by $\phi = 2n - 1$. We can perform the significance test on these results, since f follows the F-distribution with the first and second degrees of freedom both being $\phi = 2n - 1$. Results at various confidence levels are given in both tables with 0 meaning that statistically significant reduction of variance occurred by the laterally heterogeneous model. For events K4, S12 and L22, the decrease of

Downloaded from http://gji.oxfordjournals.org/ at California Institute of Technology on November 7, 2014

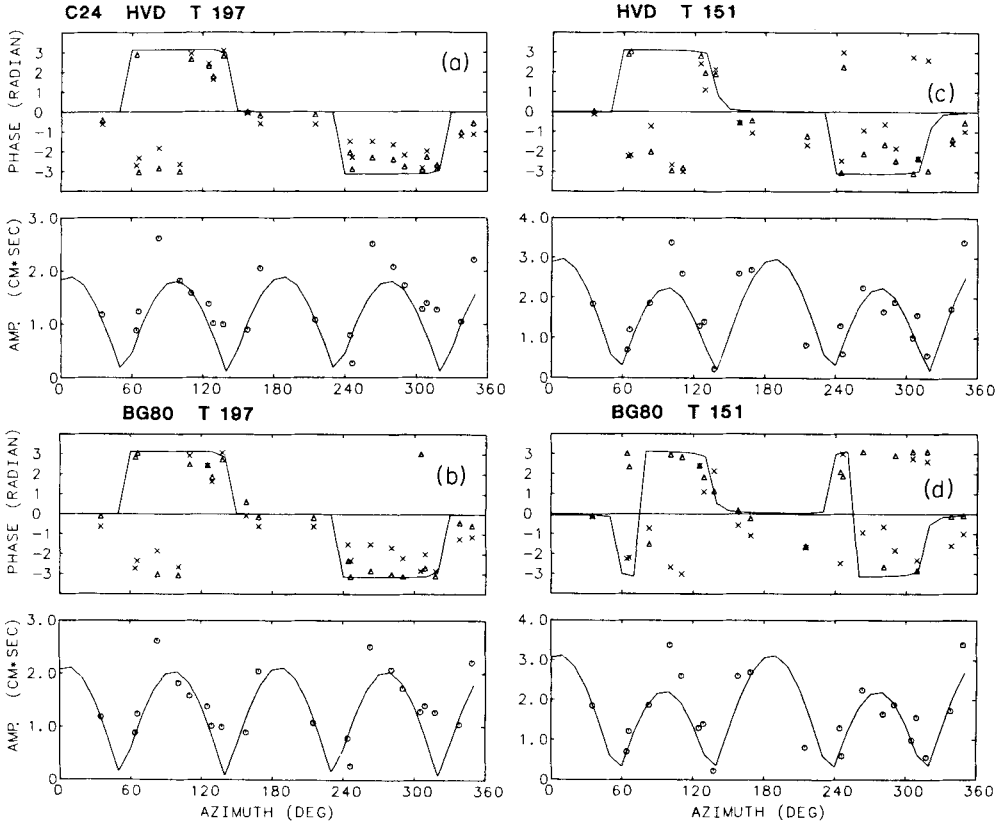

Figure 8. (a–d) Same as Fig. 7 except for a different event, C24.

Table 5. Spherical harmonic coefficients of lateral variations of Rayleigh waves. Two models, HVD and BG80, at periods 150, 200 and 250 s are shown. Their units are in per cent.

			HVD 150 SEC	BG 150 SEC	HVD 200 SEC	BG 200 SEC	HVD 250 SEC	BG 250 SEC
0	0	C	.05639	.09427	-.00131	.03458	-.01291	.01167
1	0	C	.05347	-.06128	-.01672	-.06898	-.06689	-.15999
1	1	C	.15697	.32259	.11744	.14967	.06856	.14164
1	1	S	.03491	.00658	-.00585	.03151	-.02745	-.07938
2	0	C	-.02005	.01720	-.06603	-.02478	-.10492	-.16043
2	1	C	-.09058	-.15972	-.09496	-.08783	-.09018	-.17769
2	1	S	.00363	.05047	.00991	.05999	-.01381	.05179
2	2	C	.14013	.25067	.09657	.17079	.07756	.17523
2	2	S	-.10779	-.17139	-.19594	-.23566	-.21721	-.21232
3	0	C	.11232	.20399	.10436	.07855	.07850	-.01366
3	1	C	.11183	.26334	.06837	.12878	.04517	.01712
3	1	S	.04590	.11584	.03722	.09988	.02334	.12030
3	2	C	.03044	.21209	.04549	.15447	.04979	.12276
3	2	S	-.02282	-.02098	-.03473	.00812	-.04251	-.02626
3	3	C	.02230	.17966	.07262	.15163	.06587	-.03569
3	3	S	-.06262	-.12786	-.06819	-.05754	-.06728	.03896
4	0	C	-.01589	-.12519	-.02081	-.09022	-.02206	-.00630
4	1	C	-.01811	-.04978	-.01238	.09047	.01153	.12172
4	1	S	.02726	.00392	-.00133	.03638	-.00673	-.02619
4	2	C	-.04361	-.09134	-.03278	.05079	-.00895	.02266
4	2	S	.05545	.12247	.02259	.07991	.00694	-.01598
4	3	C	-.10923	-.11046	-.04686	-.18745	-.01796	-.07835
4	3	S	-.01535	-.06330	-.01299	.01960	-.00160	-.03474
4	4	C	.05223	.03637	.02102	.08108	-.00075	.02275
4	4	S	.03813	.00974	.01590	-.04726	-.00088	-.02812
5	0	C	-.07746	.01266	-.00801	.06212	.03037	.00843
5	1	C	.25153	.26545	.17610	.11107	.10525	.16343
5	1	S	.07127	.00011	.04975	.11580	.03188	.03041
5	2	C	-.16397	-.00850	-.08941	-.01075	-.04117	-.24891
5	2	S	.13023	-.13389	.16091	-.00257	.13338	.06940
5	3	C	-.05427	-.05082	-.03297	.03330	-.01860	.00777

Downloaded from http://gji.oxfordjournals.org/ at California Institute of Technology on November 7, 2014

Table 5 – *continued*

			HVD 150 SEC	BG 150 SEC	HVD 200 SEC	BG 200 SEC	HVD 250 SEC	BG 250 SEC
5	3	S	.12010	-.11498	.06343	-.04231	.02625	-.02724
5	4	C	.11408	.09285	.05319	.06463	.00447	-.06920
5	4	S	-.20748	-.10404	-.13659	-.01060	-.07445	-.04116
5	5	C	.03518	-.04358	.03919	.12907	.03124	.12940
5	5	S	.03094	-.14805	.02018	-.11459	.00662	-.08036
6	0	C	-.06051	.04793	-.07071	-.13606	-.06299	-.03893
6	1	C	-.01868	-.00287	-.00992	.02154	-.00167	-.01830
6	1	S	-.06110	-.06326	-.04810	-.01306	-.03487	.10785
6	2	C	-.05879	-.15059	-.02946	.03179	-.00876	-.12040
6	2	S	.02907	.13074	-.00727	.05002	-.00723	.07908
6	3	C	-.01440	-.15710	-.02127	-.16466	-.01855	-.10141
6	3	S	.08096	.05874	.05926	.05044	.03892	-.01326
6	4	C	-.03171	-.00750	-.05466	-.07701	-.05460	.02320
6	4	S	.10638	.11739	.08833	.05212	.05659	.04248
6	5	C	.10322	.06998	.08229	.12942	.06511	.00322
6	5	S	.12317	.16166	.07883	.09481	.04752	.12900
6	6	C	-.00973	-.01920	.04241	-.02073	.04786	.01142
6	6	S	.04719	-.00149	.02022	.00444	-.00012	.00609
7	0	C	-.02212	-.01500	.00154	.06183	.01466	.09723
7	1	C	.02053	-.12183	.02957	.05104	.02528	.09044
7	1	S	.08595	.13165	.03588	.13091	.00588	.12487
7	2	C	-.05349	-.03804	-.05512	.04716	-.04505	-.20445
7	2	S	.01907	-.06317	-.02645	-.06078	-.03479	.07358
7	3	C	.05950	-.08901	.04526	.04066	.03245	-.10820
7	3	S	.16474	-.02262	.13341	-.09467	.08784	-.05941
7	4	C	.05817	-.16799	.04201	-.02087	.03225	-.00764
7	4	S	-.08307	.02878	-.08147	-.01627	-.06039	.05233
7	5	C	.01129	-.10542	.02458	.07316	.02055	-.02405
7	5	S	-.03194	.08139	-.00818	-.01348	.00241	.19515
7	6	C	.10051	-.07364	.06316	-.04839	.03571	.04747
7	6	S	-.01439	-.01922	.02775	-.14355	.03900	.00067
7	7	C	-.01743	.01156	-.00548	.11499	.00132	.09544
7	7	S	.06548	-.11627	.04391	-.07042	.03040	-.11848
8	0	C	-.02534	-.08199	-.02333	-.05050	-.01941	-.00100
8	1	C	-.01142	-.00609	-.01422	.05570	-.00952	.17041
8	1	S	-.02030	.07502	-.00189	.01940	.00536	.03564
8	2	C	-.02482	-.04328	.00605	.09956	.01234	.04600
8	2	S	.01446	-.01289	.00332	-.00144	.00174	-.11203
8	3	C	-.02268	-.12730	-.01603	-.04973	-.00371	-.04885
8	3	S	.00920	-.03705	.02035	-.09123	.01931	-.17720
8	4	C	.00239	.10047	-.01668	.00849	-.02323	.11233
8	4	S	.06313	.05038	.06247	.05740	.03790	.00836
8	5	C	-.01255	-.03356	-.00021	-.02727	.00436	-.00335
8	5	S	.03595	-.04982	.01104	.00228	-.00517	.15748
8	6	C	-.07127	-.04453	-.07849	.06759	-.06902	-.10997
8	6	S	-.01308	-.03040	.02723	-.02321	.04499	.04720
8	7	C	.02555	.14465	.01689	-.01778	.00109	.07972
8	7	S	.00727	.01441	.03067	.04496	.03317	-.15359
8	8	C	.06005	-.03023	.03238	-.00463	.01075	.00722
8	8	S	.03710	.10744	.01550	.11994	.00877	.08808
9	0	C	.00000	.06455	.00000	.05078	.00000	-.03906
9	1	C	.00000	-.19956	.00000	-.11733	.00000	-.02131
9	1	S	.00000	-.22359	.00000	-.12632	.00000	.07903
9	2	C	.00000	-.01544	.00000	.00777	.00000	-.00554
9	2	S	.00000	-.07657	.00000	-.03882	.00000	.02880
9	3	C	.00000	.06998	.00000	-.08860	.00000	.04376
9	3	S	.00000	-.11989	.00000	-.07270	.00000	-.19284
9	4	C	.00000	-.06733	.00000	-.00113	.00000	-.02541
9	4	S	.00000	-.10254	.00000	-.10542	.00000	-.15797
9	5	C	.00000	-.06701	.00000	.04648	.00000	-.08036
9	5	S	.00000	.04871	.00000	.05821	.00000	.01615
9	6	C	.00000	-.16972	.00000	-.20401	.00000	-.25737
9	6	S	.00000	.15098	.00000	.05749	.00000	.06935
9	7	C	.00000	-.04283	.00000	-.04075	.00000	-.05518
9	7	S	.00000	.10749	.00000	.03741	.00000	-.08858
9	8	C	.00000	.25205	.00000	.12980	.00000	.08808
9	8	S	.00000	.06944	.00000	.10203	.00000	-.24345
9	9	C	.00000	.09134	.00000	.06751	.00000	-.01712
9	9	S	.00000	.08182	.00000	-.00942	.00000	-.00092
10	0	C	.00000	-.02008	.00000	-.05792	.00000	-.02133
10	1	C	.00000	.03010	.00000	.02227	.00000	.18792
10	1	S	.00000	-.13234	.00000	-.12284	.00000	-.00421
10	2	C	.00000	-.05013	.00000	-.05943	.00000	.00841
10	2	S	.00000	-.03746	.00000	.04021	.00000	.07726
10	3	C	.00000	-.07859	.00000	-.02727	.00000	-.02746
10	3	S	.00000	.12458	.00000	-.03762	.00000	-.03364
10	4	C	.00000	.04522	.00000	-.06360	.00000	-.00140
10	4	S	.00000	-.02771	.00000	-.06958	.00000	-.13530
10	5	C	.00000	.02691	.00000	-.05035	.00000	-.01263
10	5	S	.00000	-.06356	.00000	.00301	.00000	.06930
10	6	C	.00000	.10344	.00000	.07766	.00000	.00640
10	6	S	.00000	.00217	.00000	.00697	.00000	.11754
10	7	C	.00000	.04539	.00000	.00795	.00000	.01152
10	7	S	.00000	.04578	.00000	.06558	.00000	-.00735
10	8	C	.00000	.05460	.00000	.00160	.00000	.10731
10	8	S	.00000	-.02053	.00000	.02665	.00000	.03353
10	9	C	.00000	-.12596	.00000	-.03812	.00000	-.14002
10	9	S	.00000	.04487	.00000	.00080	.00000	-.00121
10	10	C	.00000	-.02559	.00000	-.05151	.00000	-.00899
10	10	S	.00000	.00111	.00000	.02604	.00000	-.02416

Downloaded from http://gji.oxfordjournals.org/ at California Institute of Technology on November 7, 2014

variances is not statistically significant by the two models. One should note, however, that even for these events f is always larger than 1. For other events, we can safely conclude that variances become smaller by the two models. However, it is hard to say which of the laterally heterogeneous models is better from these results, because for some events f becomes larger for HVD while for others f is smaller for BG80.

In Figs 4(a, b) and 5(a, b), we give the phase and amplitude data of two events, Idaho and C24, at 256 s. Figs 4(a) and 5(a) are the results by the model HVD and Figs 4(b) and 5(b) are those by BG80. In each figure, the phase is shown at the top and the amplitude at the bottom. Solid lines are theoretical variations of the final results in each case. Our main interest in this paper is the phase. For a comparison of homogeneous and heterogeneous cases, we plotted the phase in an homogeneous earth by X and that in an heterogeneous earth by Δ. It is clear that the change of phase from the homogeneous case to the heterogeneous case is systematic and in general Δ is closer to $-\pi$ or π in Fig. 4(a, b) and to $-\pi$, 0 or π in Fig. 5(a, b). These changes are in the right direction, because for those shallow events the phase is either $-\pi$ or π for dip-slip events and is $-\pi$, 0 or π for strike-slip events.

5.2 RESULTS AT 197 AND 151 S

For three events, Coalinga, Idaho and C24, we did the inversions at shorter periods, 197 and 151 s. The orientations of the fault planes did not change very much at these periods from those at 256 s. Our example of the Idaho event using model BG80 is shown in Fig. 6. The changes in dip, slip and strike are about 5° in these cases and are not so significant considering the differences among different studies. This is again probably because the constraints from first motion data are great.

The values of f and the results of significant tests are given in Table 4. Variances in a heterogeneous case become much smaller than those in an homogeneous case. The reductions of variances seem comparable to the results at 256 s.

But the scatter in phase spectra is much more at 197 and 151 s than at 256 s. The phase and amplitude data of Idaho event are given in Fig. 7(a–d) and those of C24 are given in Fig. 8(a–d). Scatter at 151 s is especially large and the inversion method marginally works at this period. It is also apparent from these figures that some phases are corrected in the wrong direction. At 151 s, quite a large path deviation from the great circle path may be occurring. At 197 s, situations are simpler and the procedure of correcting phase along the great circle paths seems to work better. We examined spectra at 100 s too, but the scatter of phase is even more severe than that at 151 s. It seems that the assumption of propagation along the great circle paths is not valid below 150 s.

6 Conclusions

A method to invert the surface wave spectra with *P*-wave first motion data in a linear programming approach is developed. Instability of moment tensor inversion for shallow sources is naturally avoided by incorporation of first motion data. The inversion process, once surface wave spectra and first motion data are supplied, is completely automated and derives a solution as the minimum of L1 norm. Results of eight earthquakes demonstrate that the method works nicely in various situations.

Using this method, two recent 3-D upper mantle models are compared by applying corresponding laterally heterogeneous phase velocity variations to the inversion. At 256 s, all eight events showed smaller residuals when laterally heterogeneous models are used. Statistical tests showed, however, that only five events passed the significance test at high

Downloaded from http://gji.oxfordjournals.org/ at California Institute of Technology on November 7, 2014

confidence level and other events gave marginal reductions of variances. For three events, we examined the results at shorter periods, 197 and 151 s. At these periods, the three events showed a clear reduction of variances in a heterogeneous earth from an homogeneous earth, comparable to those at 256 s. It confirms that the two laterally heterogeneous upper mantle models we used, are improvements over the previous laterally homogeneous model (PREM), although we cannot say which of the two models is better from the present results. Scatter in phase spectra of surface wave data at shorter periods, especially at 151 s, suggests that deviation of propagation paths from the great circle paths is not negligible and these effects must be included in the analysis.

Acknowledgments

This research was supported by the Earth Sciences Section, National Science Foundation grant number CEE-8303647. Contribution number 4165, Division of Geological and Planetary Sciences, California Institute of Technology.

References

Aki, K. & Patton, H., 1978. Determination of seismic moment tensor using surface waves, *Tectonophys.*, **49**, 213–222.

Armstrong, R. D. & Hultz, J. W., 1977. An algorithm for a restricted discrete approximation in the L1 norm, *J. Soc. ind. appl. Math. numer. Anal.*, **14**, 555–565.

Bartels, R. H. & Conn, A. R., 1980. Linearly constrained discrete l2 problems, *ACM Trans. math. Softw.*, **6**, 594–608.

Bloomfield, P. & Steiger, W. L., 1984. Least absolute deviations, in *Theory, Applications, and Algorithms*, Birkhauser.

Conn, A. R. & Pietrzykowski, T., 1977. A penalty-function method converging directly to a constrained optimum, *J. Soc. ind. appl. Math. numer. Anal.*, **14**, 348–375.

Dziewonski, A. M. & Anderson, D. L., 1981. Preliminary Reference Earth Model (PREM), *Phys. Earth planet. Int.*, **25**, 297–356.

Dziewonski, A. M., Franzen, J. E. & Woodhouse, J. H., 1984. Centroid-moment tensor solutions for October–December, 1983, *Phys. Earth planet. Int.*, **34**, 129–136.

Dziewonski, A. M. & Woodhouse, J. H., 1983. An experiment in synthetic study of global seismicity: centroid-moment tensor solutions for 201 moderate and large earthquakes of 1981, *J. geophys. Res.*, **88**, 3207–3271.

Kanamori, H., 1983. Use of long-period surface waves for fast evaluation of tsunami potential of large earthquakes, *Open-file Rep. U.S. geol. Surv.. 83-525*, 148–151.

Kanamori, H. & Dziewonski, A. M., 1984. Spatio-temporal variation of seismic stress release along subduction zones, *EOS*, **65**, 235.

Kanamori, H. & Given, J. W., 1981. Use of long-period surface waves for rapid determination of earthquake-source parameters, *Phys. Earth planet. Int.*, **37**, 8–31.

Luenberger, D. G., 1984. *Linear and Nonlinear Programming*, 2nd edn, Addison-Wesley.

Michael, A. J. & Geller, R. J., 1984. Linear moment tensor inversion for shallow thrust earthquakes combining first- motion and surface wave data, *J. geophys. Res.*, **89**, 1889–1897.

Nakaniski, I. & Kanamori, H., 1982. Effect of lateral heterogeneity and source procress time on the linear moment tensor inversion of long-period Rayleigh waves, *Bull. seism. Soc. Am.*, **72**, 2063–2080.

Nakanishi, I. & Kanamori, H., 1984. Source mechanisms of twenty-six large, shallow earthquakes $M_S > 6.5$ during 1980 from *P*-wave first motion and long-period Rayleigh wave data, *Bull. seism. Soc. Am.*, **74**, 805–818.

Patton, H., 1980. Reference point equalization method for determing the source and path effects of surface waves, *J. geophys. Res.*, **85**, 821–848.

Scott, D. R. & Kanamori, H., 1985. On the consistency of moment tensor source mechanisms with first-motion data *Phys. Earth planet. Int.*, submitted.

Solomon, S. C. & Julian, B. R., 1974. Seismic constraints on ocean-ridge mantle structure: anomalous fault-plane solutions from first motions, *Geophys. R. J. astr. Soc.*, **38**, 265–285.

Downloaded from http://gji.oxfordjournals.org/ at California Institute of Technology on November 7, 2014

Tanimoto, T., 1985. The Backus–Gilbert approach to the three-dimensional structure in the upper mantle – I. Lateral variation of surface wave phase velocity with its error and resolution, *Geophys. J. R. astr. Soc.*, **82**, 105–123.

Tanimoto, T. 1986. The Backus–Gilbert approach to the 3-D structure in the upper mantle – II. *SH* and *SV* velocity, *Geophys. J. R. astr. Soc.*, **84**, 49–69.

Trehu, A., Nabelek, J. L. & Solomon, S. C., 1981. Source characterization of two Reykjanes ridge earthquakes: surface waves and moment tensors, *P* waveforms and nonorthogonal nodal planes, *J. geophys. Res.*, **86**, 1701–1724.

Woodhouse, J. H. & Dziewonski, A. M., 1984. Mapping the upper mantle: three-dimensional modelling of earth structure by inversion of seismic waveforms, *J. geophys. Res.*, **89**, 5953–5986.

Downloaded from http://gji.oxfordjournals.org/ at California Institute of Technology on November 7, 2014